Electronic Supplementary Material (ESI) for Analyst.
This journal is © The Royal Society of Chemistry 2020

Supporting Information

In Situ Multiplex Detection of Serum Exosomal MicroRNAs Using All-in-One Biosensor for Breast Cancer Diagnosis

Huizhen Wang, [a] *Dinggeng He,* [a] *Kejing Wan,* [a] *Xiaowu Sheng,* [b] *Hong Cheng,* [a] *Jin Huang,* [a] *Xiao Zhou,** [b] *Xiaoxiao He** [a] *and Kemin Wang** [a]

[a]State Key Laboratory of Chemo/Biosensing and Chemometrics, College of Biology, College of Chemistry and Chemical Engineering, Hunan University, Key Laboratory for Bio-Nanotechnology and Molecule Engineering of Hunan Province, Changsha 410082, China

[b]Hunan Branch Center, National Tissue Engineering Center of China, Central Laboratory, Hunan Cancer Hospital and The Affiliated Cancer Hospital of Xiangya School of Medicine, Central South University, Changsha, Hunan Province, China

* E-mail address: xiaoxiaohe@hnu.edu.cn, cccdon@163.com, kmwang@hnu.edu.cn.

Table S1. Oligonucleotides used in this work.[a]

Name	Sequence (from 5 to 3)
Y1	GGGTG GCGAG AGCGA CGATC CCTCA ACATC AGTCT GATAA GCTA-BHQ-1
Y2	GGGAT CGTCG CAGAG TTGAC CCTCG GAACT TAGCC ACTGT GAA-BHQ-2
Y3	GGGTC AACTC TTCTC GCCAC CCTCA CGCGA GCCGA ACGAA CAAA-BHQ-2
RP-21	FAM-TAGCT TATCA GAC
RP-27a	Cy3-TTCAC AGTGG CT
RP-375	Cy5-TTTGT TCGTT CGG3
Synthetic miR-21	TAGCT TATCA GACTG ATGTT GA
Synthetic miR-27a	TTCAC AGTGG CTAAG TTCCG C
Synthetic miR-375	TTTGT TCGTT CGGCT CGCGT GA
miR-21	UAGCU UAUCA GACUG AUGUU GA
miR-27a	UUCAC AGUGG CUAAG UUCCG C
miR-375	UUUGU UCGUU CGGCU CGCGU GA
Control RP-21	FAM-CAGAC TATTC GAT
Control Y1	GGGTG GCGAG AGCGA CGATC CCTTT TTTTT TATCG AATAG TCTG-BHQ-1
miR-141	UAACA CUGUC UGGUA AAGAU GG
miR-200b	UAAUA CUGCC UGGUA AUGAU GA
let-7d	AGAGG UAGUA GGUUG CAUAG UU
Control target	NNNNN NNNNN NNNNN NNNNN NN

Table S2. Comparison of different methods for detecting exosomal miRNAs.

Method	LOD	Reproducibility	Stability	Time	Marker	Ref.
Polymeride-ECL method	10^2 (particles/μL)	N/A	N/A	3–5	Protein, miR-21	1
Molecular beacons and fluorescent dye-conjugated antibodies-based method	10^7 (particles/μL)	N/A	N/A	5	Protein, miR-21	2
Molecular beacons-based method	N/A	N/A	N/A	1	miR-21, miR-27, miR-375	3
Hybridization chain reaction and DNAzyme-based amplification	10 pM	N/A	N/A	2	miR-21	4
In situ based on Au nanoflare probe	0.68 nM	N/A	N/A	4	miR-1246	5
Magneto-plasmonic nanomaterial-based amplification method	1 pM	N/A	N/A	1.5	miR-124	6
Amplification-free electrochemical detection	1 pM	Low (<5.5%)	N/A	N/A	miR-21	7
Surface-enhancement Raman scattering analysis strategy	5 fM	N/A	N/A	1	miR-21	8
Ratiometric fluorescent bioprobe based amplification method	3 fM	N/A	Good	2	miR-21	9
A ratiometric electrochemical biosensor	67 aM	Medium (3.21% and 4.47%)	Good	> 0.7	miR-21	10
Amplification-free ratiometric electrochemical detection	2.3 fM	Good (2.15%)	Good	1.5	miR-21	11
Microfluidics chips based on ion-exchange nanomembrane RNA sensing (Microfluidics)	2 pM	N/A	N/A	~1.5	miR-550	12
TiO_2 NSs@MoS_2 QDs-based self-powered biosensing	5 fg/mL	Medium (<2.3%)	Good	2	HOTTIP	13
All-in-one biosensor based on DNA three-way junction	0.116 μg/mL, 0.125 μg/mL, 0.287 μg/mL	Good (0.96%)	Good	0.5	miR-21, miR-27, miR-375	**This Work**

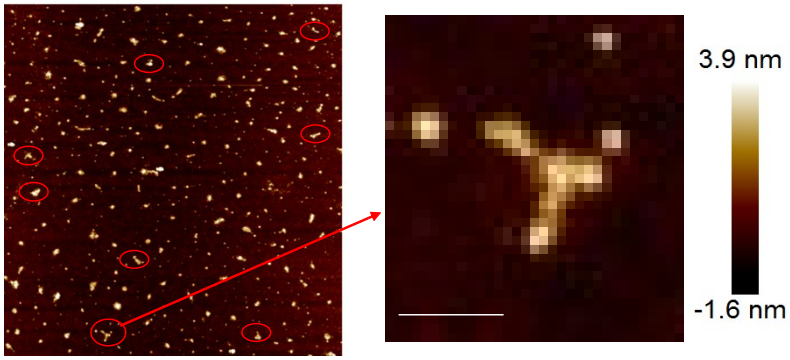

Fig. S1 AFM image of all-in-one biosensor. Right: enlarge image (Scale bar: 10 nm).

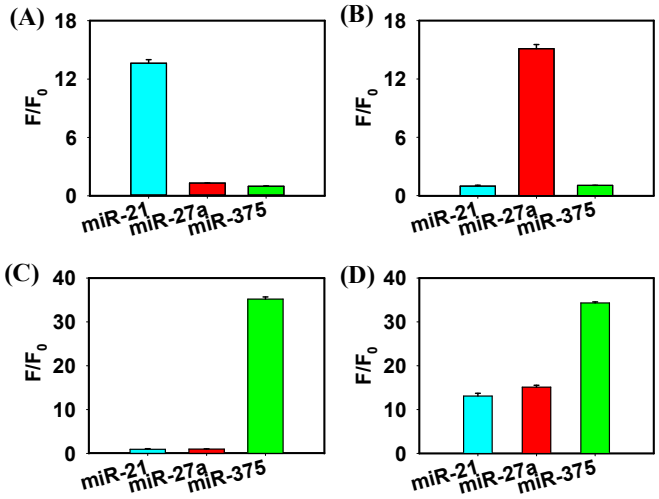

Fig. S2 Fluorescence intensities of all-in-one biosensor incubated with miR-21 (A), miR-27a (B), miR-375 (C) and three miRNAs (miR-21, miR-27a and miR-375) (D), respectively. All values are mean ± SD (n=3).

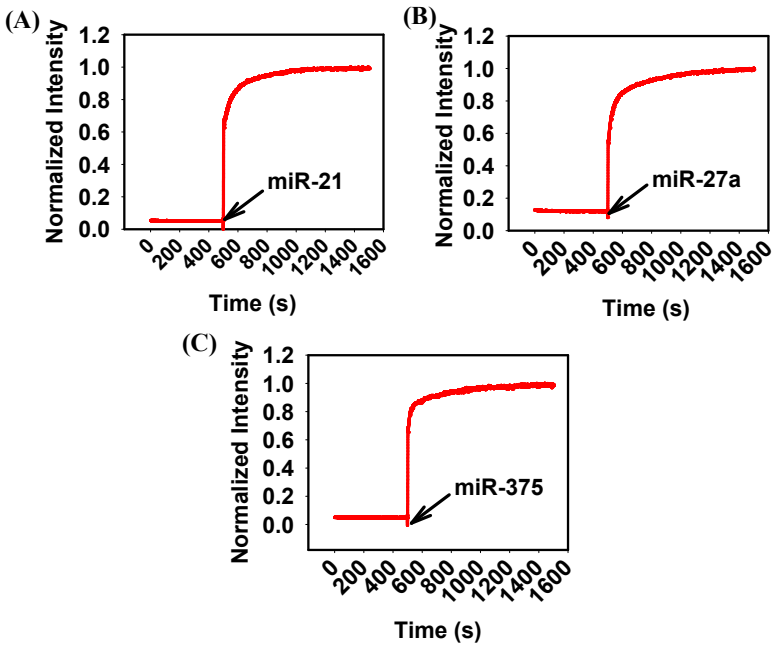

Fig. S3 Kinetic studies of the all-in-one biosensor incubated with synthetic miR-21 (A), miR-27a (B) and miR-375 (C), respectively. Arrow denoted the additional miRNA targets.

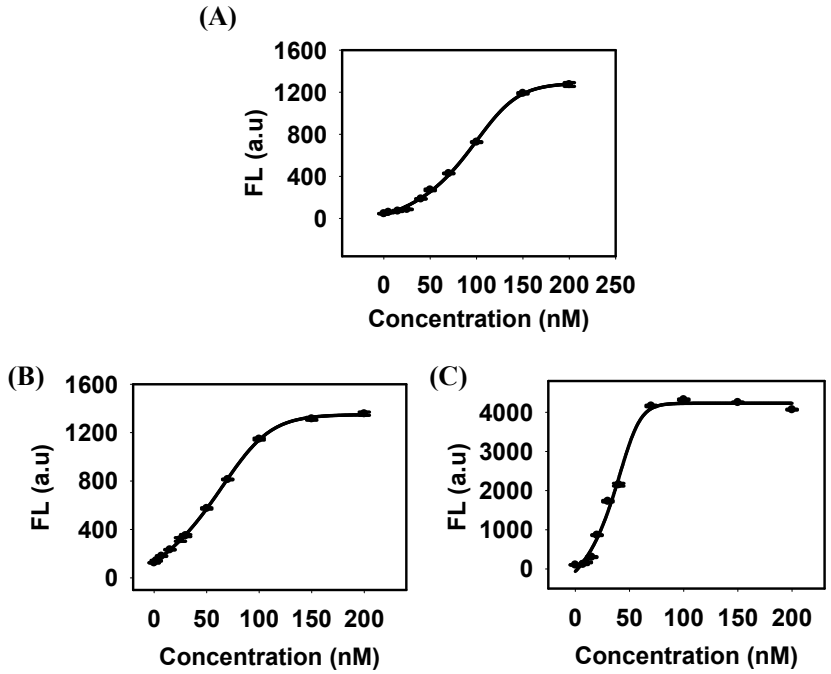

Fig. S4 Fluorescence intensities of biosensor over various concentrations of miR-21 (A), miR-27a (C) and miR-375 (E) in a concentration-dependent manner. All values are mean ± SD (n=3).

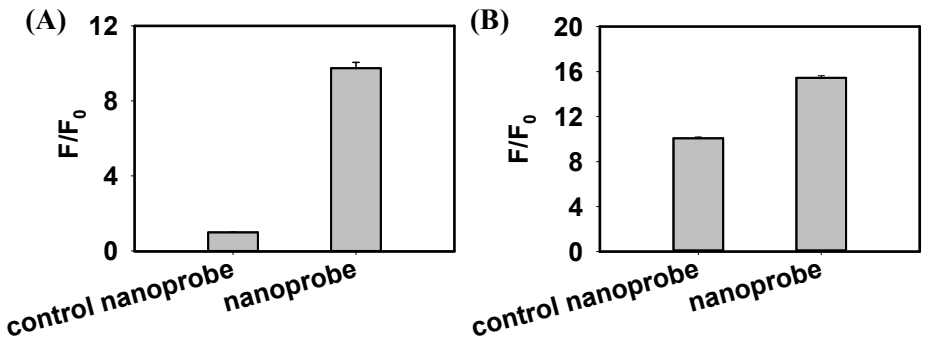

Fig. S5 Specificity studies of all-in-one biosensor and control biosensor toward miR-21 (A) and exosomal miR-21 (B), respectively. All values are mean ± SD (n=3).

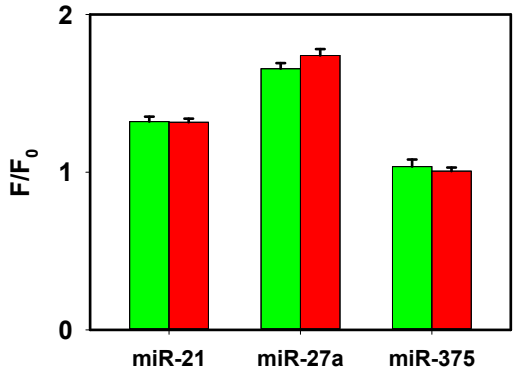

Fig. S6 Applicability of the biosensor in the presence of nontargets miRNA. 100 nM of biosensor was incubated with three target miRNAs (5 nM) (green bar). 100 nM of biosensor was incubated with three target miRNA (5 nM) and three nontargets miRNAs including miR-200b, miR-141 and let 7d (100 nM) (red bars). All values are mean ± SD (n=3).

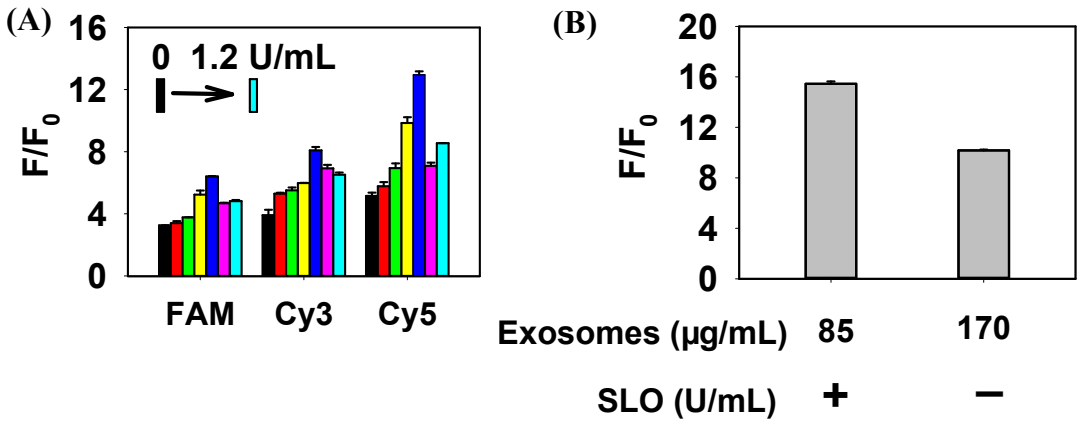

Fig. S7 (A) Optimization of SLO concentrations ranging from 0 to 1.2 U/mL for the best delivery of biosensor into exosomes (85 μg/mL). (B) Investigation of the enhanced delivery of biosensor into exosomes with aid of SLO at an optimum concentration of 0.8 U/mL. All values are mean ± SD (n=3).

We optimized the concentrations of SLO to obtain higher fluorescence recoveries. In the presence of equal concentrations of exosomes, fluorescence signals from the hybridization between the biosensor and three exosomal miRNAs significantly increased with various concentrations of SLO ranging from 0 to 1.2 U/mL and reached a plateau at 0.8 U/mL. Thus, we selected 0.8 U/mL of SLO for the following experiments.

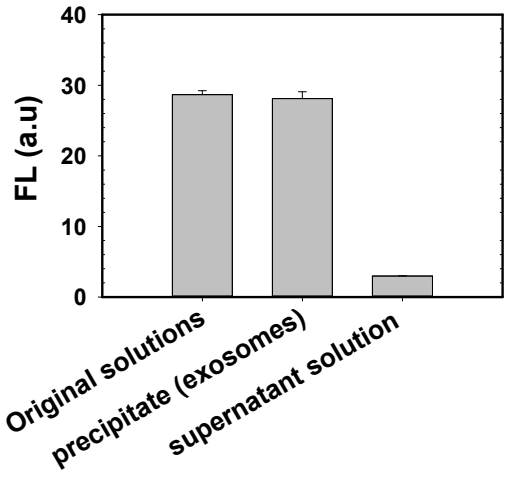

Fig. S8 Investigation of the effect of SLO treatment on the leakage of exosomal miR-21 by ultracentrifugation. All values are mean ± SD (n=3).

To rule out these possibilities, the SLO-treated exosomes were isolated by ultracentrifugation (100000, 4h). Taking the detection of exosomal miR-21 as an example, we then measured the fluorescence intensities from isolated exosomes and supernatant solutions, respectively. Notably, a relatively lower fluorescence intensity was generated from the supernatant solutions. In contrast, the precipitates (exosomes) also displayed a strong fluorescence when compared with the original solutions (Fig. S8). These results suggested that almost none of miR-21 were leaked from exosomes after SLO treatment and the hybridization reaction of biosensor and miR-21 was happened inside exosomes rather than outside of the exosomes.

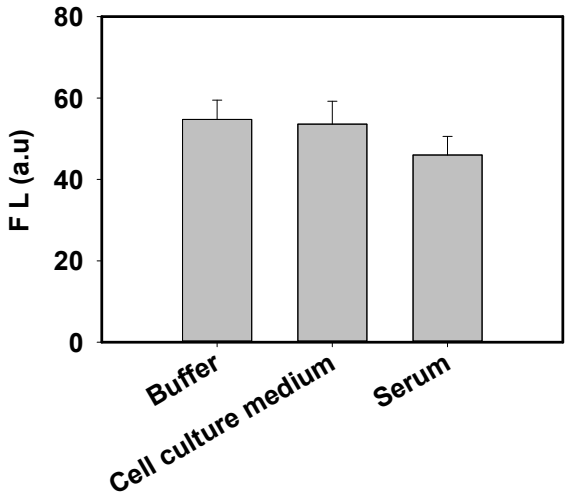

Fig. S9 Stability of the biosensor in Tris-HCl buffer, cell culture medium and serum (60 %) for 2 h, respectively. All values are mean ± SD (n=3).

Reference

[1] Z. Fan, J. Yu, J. Lin, Y. Liu and Y. Liao, *Analyst*, **2019**, 144, 5856-5865.

[2] S. Cho, H. C. Yang and W. J. Rhee, *Biosens. Bioelectron*., **2019**, 146, 111749.

[3] J. H. Lee, J. A. Kim, S. Jeong and W. J. Rhee, *Biosens. Bioelectron*., **2016**, 86, 202-210.

[4] D. He, L. Hai, H. Wang, R. Wu and H. W. Li, *Analyst*, **2018**, 143, 813-816.

[5] L.Y. Zhai, M. X. Li, W. L. Pan, Y. Chen, M. M. Li, J. X. Pang, L. Zheng, J. X. Chen and W. J. Duan, *ACS. Appl. Mater. Interface*., **2018**, 10, 39478-39486.

[6] J. Lee, J. Choi, S. D. Chueng, T. Pongkulapa, L. Yang, H. Cho, J. Choi and K. Lee, *ACS Nano*, **2019**, 13, 8793-8803.

[7] K. Boriachek, M. Umer, M. N. Islam, V. Gopalan, A. K. Lam, N. T. Nguyen and M. J. A. Shiddiky, *Analyst*, **2018**, 143, 1662-1669.

[8] D. Ma, C. Huang, J. Zheng, J. Tang, J. Li, J. Yang and R. Yang, *Biosens. Bioelectron*., **2018**, 101 167-173.

[9] Y. Xia, L. Wang, J. Li, X. Chen, J. Lan, A. Yan, Y. Lei, S. Yang, H. Yang and J. Chen, *Anal. Chem*. **2018**, 90, 8969-8976.

[10] J. Zhang, L. L. Wang, M. F. Hou, Y. K. Xia, W. H. He, A, Yan, Y. P. Weng, L. P. Zeng and J. H. Chen, *Biosens. Bioelectron*., **2018**, 102, 33-40.

[11] L. Luo, L. Wang, L. Zeng, Y. Wang, Y. Wen, Y. Liao, T. Chen, Y. Xia, J. Zhang and J. Chen, *Talanta*, **2020**, 207, 120298.

[12] D. Taller, K. Richards, Z. Slouka, S. Senapati, R. Hill, D. B. Go and H. C. Chang, *Lab Chip*., **2015**, 15, 1656-1666.

[13] X. Pang, X. Zhang, K. Gao, S. Wan, C. Cui, L. Li, H. Si, B. Tang and W. Tan, *ACS Nano*, **2019**, 13, 1817-1827.